

Dynamic Time Over Threshold Method

Kenji Shimazoe, Hiroyuki Takahashi, Boxuan Shi, T. Orita, Tetsuo Furumiya, Junichi Ooi, and Yoshihiko Kumazawa

Abstract—The time over threshold (TOT) method has several advantages over direct pulse height analysis based on analog to digital converters (ADCs). A key advantage is the simplicity of the conversion circuit which leads to a high level of integration and a low power consumption. The TOT technique is well suited to build multi-channel readout systems for pixelated detectors as described in our previous work that also exploits the Pulse Width Modulation (PWM) method. The main limitation of the TOT technique is that the relation between the input charge to be measured and the width of the encoded pulse is strongly non-linear. Dynamic range limitation is also an issue. To address these aspects, we propose a new time over threshold conversion circuit where the threshold of the comparator is dynamically changed instead of being constant. We call this scheme the “dynamic TOT method”. We show that it improves linearity and dynamic range. It also shortens the duration of measured pulses leading to higher counting rates. We present a short analysis that explains how the ideal linear input charge to TOT transfer function can theoretically be obtained. We describe the results obtained with a test circuit built from discrete components and present several of the spectrums obtained with crystal detectors and a radioactive source. The proposed method can be used for applications like Positron Emission Tomography (PET) that require moderate energy resolution.

Index Terms—Dynamic time over threshold (TOT), positron emission tomography (PET), pulse width modulation (PWM), time over threshold (TOT).

I. INTRODUCTION

TIME over threshold (TOT) measurement systems have several advantages over conventional pulse height measurement systems based on analog to digital converters (ADCs). Circuit simplicity brings advantages to potentially reach higher levels of channel density, lower power consumption and more efficient pin-saving digital output interfaces. However, since the relation between the TOT and the charge deposited in a detector is strongly non-linear, some digital processing (for example a look-up table) is required to properly estimate energy. The limited effectiveness of elementary digital processing causes distortions in the energy spectrum and degrades energy resolution [1]–[3]. A conventional TOT circuit consists of a preamplifier-shaper-discriminator chain. The threshold of the discriminator is generally programmable but fixed after an initial setup procedure. Some systems use several comparators per channel and the

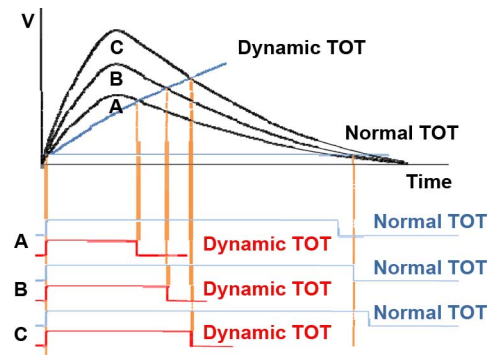


Fig. 1. Concept of the dynamic TOT method.

corresponding number of thresholds. For example, multi-level TOT systems with three or more thresholds have been reported in [4] and [5]. Using multiple thresholds improves the dynamic range at the expense of a more complicated circuit, a larger number of connections for readout and extra digital data processing. We propose a new technique called the “dynamic TOT method” to estimate pulse height (i.e., energy) from the temporal width of a pulse obtained by comparing the input signal to a dynamically changing threshold level. We show that this method can improve linearity, achieves a wide dynamic range, and also shortens pulse width which is desirable to improve count rate. We describe the concept of the method and report experimental results obtained with a prototype circuit built from discrete components coupled to several types of crystal detectors. This method can be useful for multi-channel readout applications such as Positron Emission Tomography (PET) that require moderate energy resolution.

II. DYNAMIC TOT METHOD

A. Concept of Dynamic TOT

Fig. 1 shows the concept of both the conventional TOT method and the proposed dynamic TOT method. The transfer function of TOT versus input charge depends significantly on the shape of the input pulse. For the shapes considered in this study, this relation is proved to be non-linear when a single fixed threshold is used. The proposed dynamic TOT method uses a threshold level that is varied after the pulse to be measured crosses a pre-defined initial level.

The dynamic threshold is implemented using a positive feedback from the output of the discriminator to the threshold level itself. This feedback is accomplished through a circuit that we call the “threshold function generating (TFG) module”. This module is triggered after the input signal comes over an initial threshold level. The dynamically changing threshold level ramps-up until it crosses the input signal. The time from the initial threshold crossing until the threshold reaches the input signal is the output of the dynamic TOT circuit. A simple counter is used at this level to perform the time to digital

Manuscript received February 08, 2011; revised June 07, 2012; accepted July 23, 2012. Date of publication September 20, 2012; date of current version December 11, 2012.

K. Shimazoe is with the Department of Bioengineering, The University of Tokyo, Bunkyo-Ku, Tokyo, 113-8656, Japan (e-mail: shimazoe@it-club.jp).

H. Takahashi and B. Shi are with the Department of Nuclear Engineering and Management, The University of Tokyo, Bunkyo-Ku, Tokyo, 113-8656, Japan (e-mail: leo@n.t.u-tokyo.ac.jp; shiboxuan@sophie.q.t.u-tokyo.ac.jp).

T. Furumiya, J. Ooi and Y. Kumazawa are with the Shimadzu Corporation, Kyoto, Japan (e-mail: {furumiya, ohi, kumazawa}@shimadzu.co.jp).

Color versions of one or more of the figures in this paper are available online at <http://ieeexplore.ieee.org>.

Digital Object Identifier 10.1109/TNS.2012.2215338

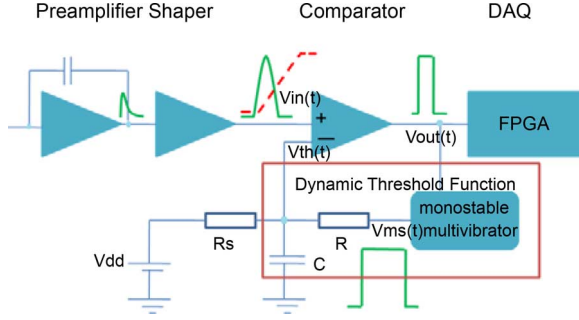


Fig. 2. Dynamic TOT test circuit.

conversion. By choosing the adequate function to generate the variable threshold, a linear relation between the input charge and TOT can be obtained. The initial threshold is set to a relatively low level, and the first crossing with the input signal can be used to derive timing information. Conventional TOT systems do not offer an optimal solution in terms of linearity of the estimated energy and precise timing. We claim that the dynamic TOT method is superior on these aspects. Further improvements can be obtained by correcting timing information using energy information as described in [6].

B. Circuit Design

Fig. 2 shows the proposed detector readout test circuit. It comprises the usual preamplifier-shaper-discriminator chain, and adds two new components: a mono-stable multi-vibrator and a TFG module. In steady state, the initial threshold level is constant. It is determined by the bias voltage V_{dd} and the resistor divider made by R_s and R . When the input signal crosses the initial threshold level, the comparator generates a trigger pulse. This pulse is delayed and widened by the mono-stable multi-vibrator circuit. The fixed-duration pulse that is obtained controls the TFG module. The output of this module is added to the initial threshold and is fed back at the input of the comparator (V_{th}). In practice, we used a simple RC network implemented with discrete components to build the TFG module.

Fig. 3 shows the signals relevant to the operation of the test circuit. The temporal sequence is as follows:

1. The amplified detector signal, $V_{in}(t)$, is under the threshold of the comparator. The threshold is constant at this time.
2. V_{in} reaches the threshold level causing the comparator to fire.
3. The mono-stable multi-vibrator is triggered by the leading edge of the comparator output. It generates a square pulse, $V_{ms}(t)$, that has a fixed amplitude and a constant duration.
4. The variable threshold voltage, $V_{th}(t)$, is generated from this square pulse.
5. The comparison of the input signal $V_{in}(t)$ and the dynamic threshold $V_{th}(t)$ create the output signal $V_{out}(t)$ of the dynamic TOT circuit.

In order to minimize system dead-time, the duration of the pulse generated by the multi-vibrator needs to be set to the duration of the pulse obtained for maximum amplitude input signals. In the experimental validation of the proposed circuit, we carefully tuned this duration and we also found that adding a delay

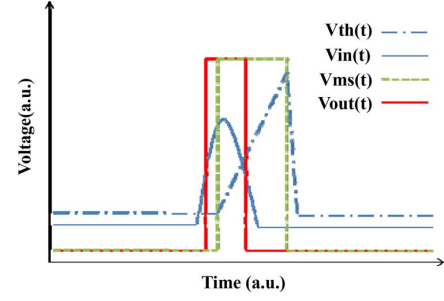


Fig. 3. Dynamic TOT signal waveforms.

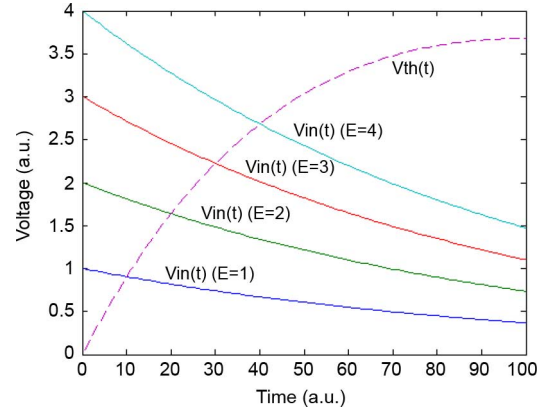


Fig. 4. Theoretical preamplifier input and ideal threshold function.

to $V_{ms}(t)$ was required to ensure that the dynamic threshold always reaches the level of the input signal after its peaking time.

The transfer function of the dynamic TOT circuit is determined by the characteristics of the threshold function and the shape of the input signal. We present some theoretical examples in the next section.

C. Dynamic TOT Without Shaping and Its Ideal Threshold Function

We assume that the shaper is bypassed and that the input signal at the positive input of the comparator is:

$$V_{in}(t) = Ee^{-t/T}. \quad (1)$$

Let E be the peak voltage to be measured and T the time constant of the corresponding charge sensitive preamplifier. The desired linear relation between the measured TOT, noted tot , and the amplitude E to be measured is:

$$E = A \frac{tot}{T}. \quad (2)$$

This linear transfer function is obtained when the threshold of the dynamic TOT circuit is:

$$V_{th}(t) = A \frac{t}{T} e^{-t/T}. \quad (3)$$

Constant A is arbitrary. We obtain a linear relation between the TOT and the input charge using the threshold function given by (3). This is shown on Fig. 4.

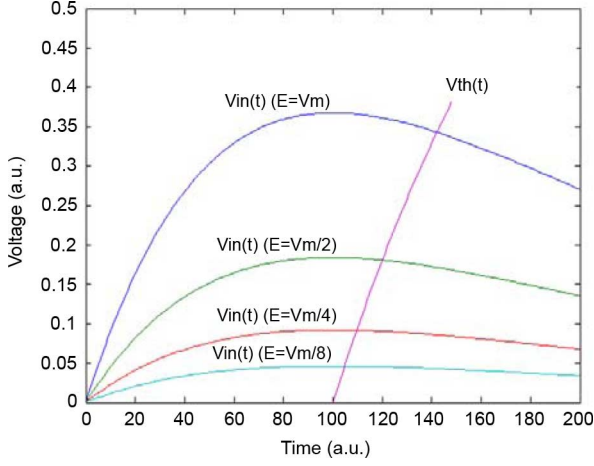


Fig. 5. Input signals after CR-RC shaper and simple RC threshold function.

D. Dynamic TOT With CR-RC Shaping and Ideal Threshold Function

We now assume that a CR-RC shaper is present. The signal from the detector that is input to the comparator is:

$$V_{in}(t) = E \left(\frac{t}{T} \right) e^{-t/T}. \quad (4)$$

The desired linear relation between E and t_{ot} given in (2) is obtained with the threshold function:

$$V_{th}(t) = A \left(\frac{t}{T} \right)^2 e^{-t/T}. \quad (5)$$

The threshold functions given in (3) and (5) are not very easy to generate in practice, but we show in the next section that a simple RC circuit can make a rather good approximation of it.

E. Dynamic TOT With CR-RC Shaping and Threshold Function Made a RC Network

In our experimental studies, we used a CR-RC shaping and a simple RC threshold function. The threshold function is:

$$V_{th}(t) = V_m \left(1 - e^{-(t-T)/T} \right) + V_{dd} \quad (t \geq T) \quad (6)$$

$$V_{th}(t) = V_{dd} \quad (t < T). \quad (7)$$

This equation corresponds to the step response of the RC circuit shown in Fig. 2 with an additional delay T equal to the time constant of the circuit.

The numerical results of Fig. 5 show input signals of different amplitudes and the threshold function $V_{th}(t)$.

Fig. 6 shows the relation between pulse height and Time over Threshold. Although the initial threshold level affects the transfer function, this effect can be compensated by changing the delay time T . The corresponding degradation of linearity (the norm of the residual) is about 2.2% and 0.7% for t/T in $[1; 1.45]$ and t/T in $[1; 1.2]$ respectively.

A linear relation between amplitude and TOT can be obtained by selecting the threshold function that is matched to the shape of the input signal. The dynamic TOT method can be applied to various other types of shaping, such as a semi-gaussian or trapezoidal. Compared to the fixed threshold TOT method, the

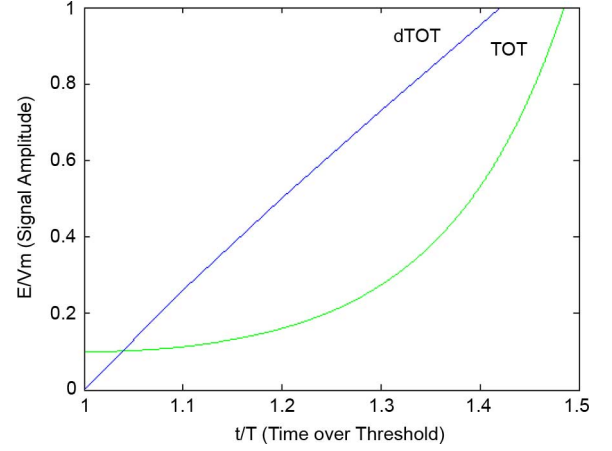


Fig. 6. Simulation of CR-RC shaping with dTOT/TOT and linearity.

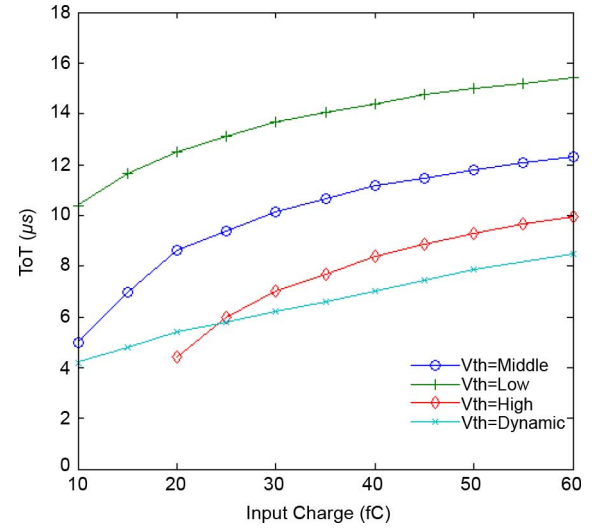


Fig. 7. Transfer function of TOT and dynamic TOT.

proposed scheme achieves superior linearity over a wider dynamic range.

III. EXPERIMENTAL RESULTS

We tested a circuit that comprises a charge sensitive preamplifier (CLEARPULSE H580), a CR-RC shaping amplifier and a comparator. The shaping time was set to $6 \mu s$. We present in Fig. 7 the measured charge to TOT transfer function obtained with three values of threshold (high, middle, and low) and a dynamic threshold generated as shown in Fig. 2. The conventional TOT method has a non-linear transfer function and strongly depends on the threshold level. The dynamic TOT method is linear over a wider dynamic range. In addition, pulses are shorter, which leads to a higher count rate when the readout of multiple channels is multiplexed as proposed in [7].

We compare on Fig. 8 the charge transfer function of the dynamic TOT circuit to that obtained by a piece-wise combination of the three transfer functions corresponding to fixed thresholds. Using three thresholds instead of one improves linearity at the expense of more complex circuitry. A linear fit was made on the dynamic TOT curve. The coefficient of determination R^2 is 0.9928 (F-test = 0.95). The measured INL (Integrated Non

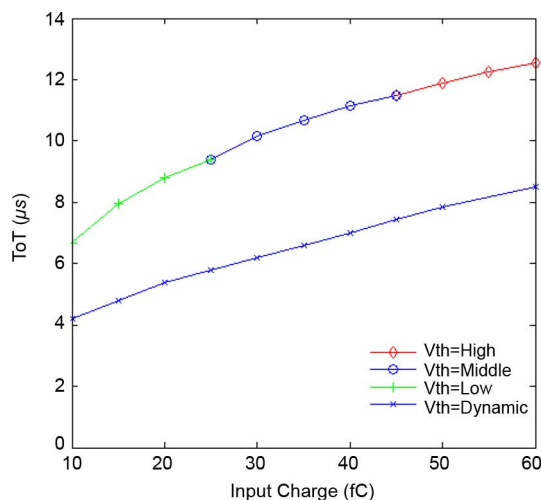


Fig. 8. Multi-Threshold TOT and dynamic TOT.

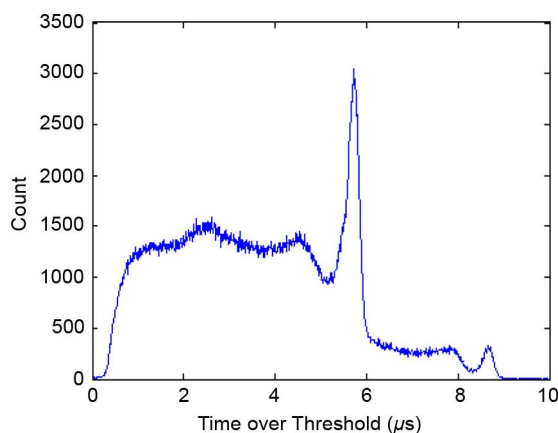


Fig. 9. Energy spectrum of LuAG-APD with dynamic TOT.

Linearity) is 4% and less than 1% from 10 fC to 60 fC and from 20 fC to 50 fC respectively.

We tested the proposed prototype circuit with a gamma detector. Fig. 9 shows the acquired energy spectrum with a $2\text{ mm} \times 2\text{ mm} \times 8\text{ mm}$ Pr 2.5%:LuAG-APD array illuminated by a ^{22}Na source. The APD is a UV-enhanced device from Hamamatsu Photonics adapted to the wavelength of the Pr:LuAG scintillator. The crystal has 18 ns and 55 ns decay time constants and the shaping time of the shaper is set to $6\text{ }\mu\text{s}$. The two peaks that are observed correspond to the 511 keV and 1.28 MeV peaks. The energy spectrum was acquired with our dynamic TOT circuit connected to a time-to-digital converter based on a counter implemented in an Altera Cyclone III FPGA clocked at 100 MHz (i.e., the least significant bit of the converter is 10 ns). Resolution was about 10 bits. Using a faster clock would improve resolution.

Fig. 10 compares the spectrum obtained with a commercial 14-bit 2 MHz ADC system to that obtained with our dynamic TOT circuit after the appropriate scaling and calibration. We applied a linear transformation followed by a re-binning on the spectrum of Fig. 9 to make its two peaks (511 keV and 1.28 MeV) coincide with those obtained with the ADC. The measured energy resolution is 12% for the ADC-based system and

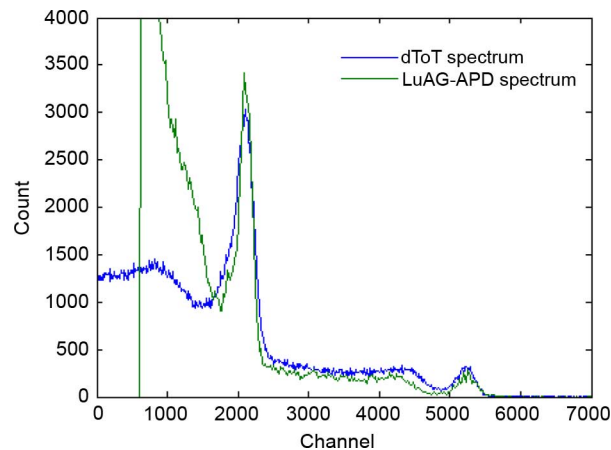


Fig. 10. Comparison between ADC pulse height analysis and dTOT.

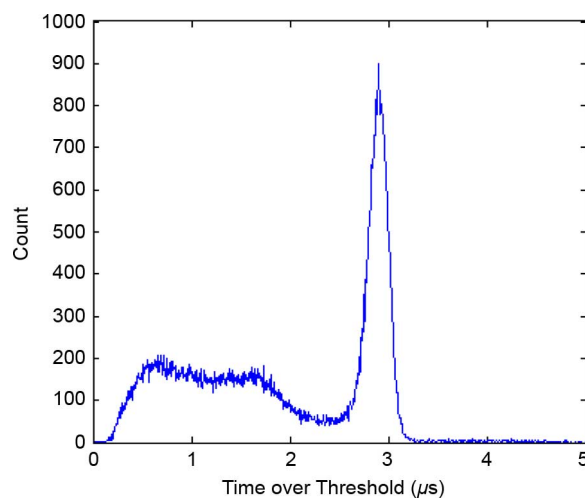


Fig. 11. Energy spectrum of NaI-PMT with dynamic TOT.

14% for the dynamic TOT circuit. The small degradation is acceptable for resolving the energy of gamma detectors, such as those used in PET systems [8]. Because the linear transform does not perform well in the low energy part of the spectrum, large distortions appear in this region. This is not an issue for applications like PET because this portion of the spectrum is outside of the area of interest, but it prevents using the proposed technique for general precision spectroscopy applications.

Fig. 11 shows the spectrum of a ^{137}Cs source obtained with a NaI-PMT detector connected to a preamplifier, semi-gaussian shaper and dynamic TOT circuit. The size of the detector is $2\text{ inch} \times 2\text{ inch}$. The peak at 662 keV and the Compton edge are clearly observed. Energy resolution is 9% at the 662 keV peak.

The spectrum of several radioisotope (^{22}Na , ^{137}Cs and ^{60}Co) was measured with this method to support the linearity data of a test pulse using an APD (S8064-55) detector couple with a GAGG crystal ($5\text{ mm} \times 5\text{ mm} \times 5\text{ mm}$) (Fig. 12). The photopeak of each radioisotope was plotted in Fig. 13. The coefficient of determination R^2 is 0.9993 with a linear fit. The INL in this range was 1.6%.

As shown, the dynamic TOT method can perform energy measurements with moderate energy resolution using a simple circuit that has a binary digital output.

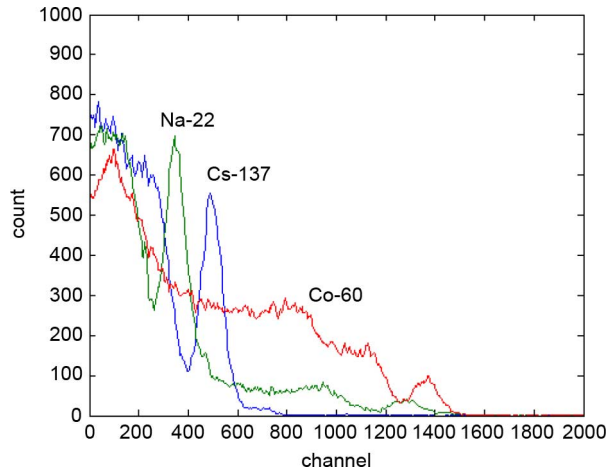


Fig. 12. Energy spectrum with ^{137}Cs , ^{22}Na and ^{60}Co .

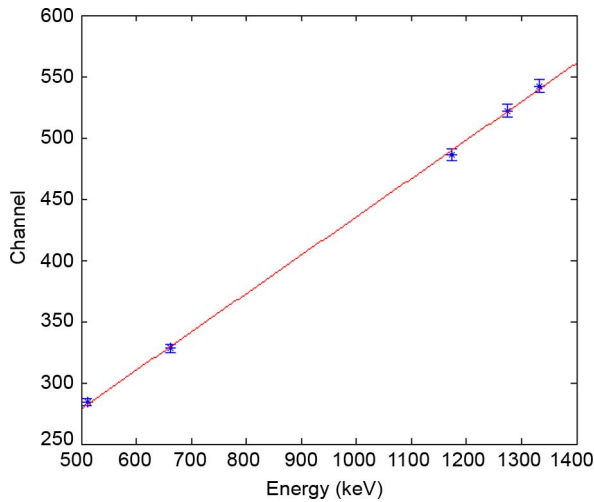


Fig. 13. Photopeak with ^{137}Cs , ^{22}Na and ^{60}Co and linear fit.

IV. DISCUSSION

In PET systems, the individual readout of each pixel is essential to achieve a high spatial resolution[9]. However, using an ADC per channel is not power efficient (e.g., ~ 120 mW per channel) and requires a large number of interface lines between the ADCs and the digital front-end electronics [10]. In contrast, the dynamic TOT circuit is simple and can easily be integrated in an ASIC. We estimate that the power consumption would be around 4 mW per channel and that the silicon area would be less than half of a comparable ADC. The number of interface lines is reduced from N to 1 when a N -bit parallel output ADC is replaced by a dynamic TOT circuit. A single digital transmission line per channel is particularly advantageous in multi-channel systems and further line count reduction can be achieved by multiplexing several channels on the same line.

V. CONCLUSION

We have proposed and tested a new method to estimate the energy of pulses in nuclear spectroscopy from the measurement of

time over threshold. The key point in our method is to compare the input signal to a dynamically changing threshold. The stability and reproducibility of the variable threshold generator are critical to achieve good performance. Although manual tuning was acceptable on our single channel prototype circuit, larger systems would require an automatic tuning and calibration capability.

Our studies and measurements show that the dynamic ToT method improves linearity over a wider dynamic range compared to the usual single fixed-threshold technique. However, the proposed technique does not outperform the linearity and dynamic range reached by conventional ADC-based systems. One of the advantages of the proposed circuit over ADC-based systems is the simplicity of its digital interface: it only requires one line to transport time and energy (represented by pulse width) information. We used our prototype circuit with several detector crystals and we think that our method is adequate for PET systems and application that require moderate dynamic range and precision.

ACKNOWLEDGMENT

This study was conducted as a part of the project “R&D of Molecular Imaging Equipment for Malignant Tumor Therapy Support,” supported by the New Energy and Industrial Technology Development Organization (NEDO).

REFERENCES

- [1] I. Kipnis, T. Collins, J. DeWitt, S. Dow, A. Frey, A. Grillo, R. Johnson, W. Kroeger, A. Leona, L. Luo, E. Mandelli, P. F. Manfredi, M. Melani, M. Momayezi, F. Morsani, M. Nyman, M. Pedrali-Noy, P. Poplevin, E. Spencer, V. Re, and N. Roe, “A time-over-threshold machine: The readout integrated circuit for the BABAR silicon vertex tracker,” *IEEE Trans. Nucl. Sci.*, vol. 44, no. 3, pp. 289–297, Jun. 1997.
- [2] T. C. Meyer, F. Powolny, F. Anghinolfi, E. Auffray, M. Dosanjh, H. Hillemanns, H.-F. Hoffmann, P. Jarron, J. Kaplon, M. Kronberger, P. Lecoq, D. Moraes, and J. Trummer, “A time-based front end readout system for PET & CT,” in *Proc. IEEE Nucl. Sci. Symp. Conf.*, Oct. 1, 2006, vol. 4, pp. 2494–2498.
- [3] J. Yeom, I. Defendi, H. Takahashi, K. Zeitelhack, M. Nakazawa, and H. Murayama, “A 12-channel CMOS preamplifier-shaper-discriminator ASIC for APD and gas counters,” *IEEE Trans. Nucl. Sci.*, vol. 53, no. 4, pp. 2204–2208, Aug. 2006.
- [4] H. Kim, C. M. Kao, Q. C. Xie, T. Chen, L. Zhou, F. Tang, H. Frisch, W. W. Moses, and W. S. Choonge, “A multi-threshold sampling method for TOF PET signal processing,” *Nucl. Instrum. Methods Phys. Res. A*, vol. 602, no. 2, pp. 618–621, Apr. 2009.
- [5] T. Fujiwara and H. Takahashi, “A new multi-level time over threshold method for energy resolving multi-channel systems,” in *Proc. IEEE NSS Conf.*, Oct. 19–25, 2008, pp. 3413–3415.
- [6] N. Matsuoka and Y. Yokota, “Leading edge timing compensation for accurate drift-time measurements in the case of resistive anode wire,” in *Proc. IEEE NSS Conf.*, 2000, vol. 1, pp. 5/84–5/85.
- [7] K. Shimazoe, H. Takahashi, B. Shi, T. Furumiyu, J. Ooi, Y. Kumazawa, and H. Murayama, “Novel front-end pulse processing scheme for PET system based on pulse width modulation and pulse train method,” *IEEE Trans. Nucl. Sci.*, vol. 57, no. 2, pp. 782–786, Apr. 2010.
- [8] J.-F. Pratte, G. De Geronimo, S. Junnarkar, P. O’Connor, B. Y. S. Robert, C. Radeka, C. Woody, S. Stoll, P. Vaska, A. Kandasamy, R. Lecomte, and R. Fontaine, “Front-end electronics for the RatCAP mobile animal PET scanner,” *IEEE Trans. Nuclear Science*, vol. 51, no. 4, Aug. 2004.
- [9] W. Moses and S. Derenzo, “Empirical observation of resolution degradation in positron emission tomographs utilizing block detectors,” *J. Nucl. Med.*, vol. 34, pp. 101–102, 1994.
- [10] K. Shimazoe, Y. Jy, H. Takahashi, T. Kojo, Y. Minamikawa, K. Fujita, and H. Murayama, “Multi-channel waveform sampling ASIC for animal PET system,” in *Proc. IEEE NSS Conf.*, Oct. 1, 2006, vol. 4, pp. 2473–2475.